Available online at www.sciencedirect.com
SCIENCE DIRECT®
International Journal of Solids and Structures 43 (2006) 1253–1275
INTERNATIONAL JOURNAL OF SOLIDS and STRUCTURES
www.elsevier.com/locate/ijsolstr

A directed continuum model of micro- and nano-scale thin films

C.L. Randow, G.L. Gray, F. Costanzo *

Engineering Science and Mechanics Department, The Pennsylvania State University, 212 Earth and Engineering Sciences Building, University Park, PA 16802, USA

Received 9 November 2004; received in revised form 22 March 2005
Available online 23 May 2005

Abstract

As is well known, classical continuum theories cease to adequately model a material's behavior as long-range loads or interactions begin to have a greater effect on the overall behavior of the material, i.e., as the material no longer conforms to the locality requirements of classical continuum theories. It is suggested that certain structures to be analyzed in this work, e.g., columnar thin films, are influenced by non-local phenomena. Directed continuum theories, which are often used to capture non-local behavior in the context of a continuum theory, will therefore be used. The analysis in this work begins by establishing the kinematics relationships for a discrete model based on the physical structure of a columnar thin film. The strain energy density of the system is calculated and used to formulate a directed continuum theory, in particular a micromorphic theory, involving deformations of the film substrate and deformations of the columnar structure. The resulting boundary value problem is solved analytically to obtain the deformation of the film in response to applied end displacements.

Keywords: Micromorphic continuum; Columnar thin films; Homogenization

1. Introduction

The goal of this work is to develop accurate models of micro- and nano-scale thin film systems possessing a certain structure. This structure may be heterogeneous (for example, a material with voids, inclusions, or pores) and/or it may not sufficiently conform to the locality requirements of classical continuum

* Corresponding author. Tel.: +1 814 863 2030; fax: +1 814 863 7967.
E-mail addresses: clr198@psu.edu (C.L. Randow), gray@engr.psu.edu (G.L. Gray), costanzo@engr.psu.edu (F. Costanzo).

0020-7683/$ - see front matter © 2005 Elsevier Ltd. All rights reserved.
doi:10.1016/j.ijsolstr.2005.03.064

mechanics. For example, the state of a body at a given point may be influenced by what happens at some distance away due to long-range interaction forces. For simplicity, we begin by constructing a discrete model of the physical system we are interested in—this discrete model incorporates the heterogeneous and non-local nature of certain micro- and nano-scale systems by adding additional elements (linear and torsional springs) to a classical Euler–Bernoulli beam model. After formulating a continuous version of the discrete model, one obtains a so-called *directed continuum* theory. The directed continuum class of theories encompasses a variety of related continuum theories, including Cosserat, micropolar, micromorphic, and couple-stress theories (Eringen, 1968, 1966; Capriz and Podio-Guidugli, 1976; Mindlin, 1964; Koiter, 1964; Toupin, 1964; Askar and Cakmak, 1968).

Before describing directed continuum theories, it is useful to consider the classical continuum theory (Truesdell and Noll, 2003). In classical continuum mechanics, a body $\mathfrak{B}$ is a space that possesses a measure, the mass distribution, and consists of particles that are mapped into Euclidean space $\mathcal{E}$. The particular mapping, called a placement, establishes the volume, configuration, and mass density of the body in physical space. As the body evolves, the placement of $\mathfrak{B}$ into $\mathcal{E}$ necessarily changes. In directed continuum theories there is an additional placement of $\mathfrak{B}$. This second placement, which occurs simultaneously with the classical placement, maps the body into another finite dimensional, smooth manifold. The points of the manifold represent a structure in addition to the structure of the body in the classical continuum sense. This additional structure is often called a microstructure or microvolume, although the prefix *micro* is not necessarily a reference to size. The deformable microstructure is represented by a vector field with the vectors typically called *directors*, hence the name *directed continuum*. It is often the case that in developing a specific directed continuum theory one relies on a discrete model that possesses easily identifiable microstructural features. The time evolution of these features are captured by the selected director fields.

With this in mind, Section 2 begins by proposing a discrete model of a thin film based on observing the physical structure of a columnar thin film. The discrete model will be used to obtain a discrete form of the strain energy and to obtain Lagrange's equations. In Section 3, the continuous set of governing equations consistent with a directed continuum theory is formulated based on the discrete equations found in Section 2. (The additional microstructure of the directed continuum consists of a vector field that describes the effect of the interacting columns in the discrete model.) The strain energy density is then calculated and used with Hamilton's principle to obtain the required boundary conditions for the boundary value problem (BVP). Section 4 briefly describes the steps used to obtain an analytical solution to the problem. Finally, Section 5 includes some sample problems that highlight the usefulness of the directed continuum formulation of the thin film problem.

2. Discrete model formulation

2.1. Defining the discrete model

Before proceeding with the formulation of a continuum model, the approach described in this work begins by defining a discrete mechanical system along with its governing equations. A similar approach has been used in the structural analysis of buildings (Bažant, 1971, 1972) and, more recently, in the analysis of lattice dynamics (Suiker et al., 2001). The process of generating a discrete model begins by observing the physical structure of a columnar thin film. For some time, experimentalists have been fabricating such films consisting of a substrate, or bulk material foundation, and an observable structure, or columns, on the surface of the substrate on the scale of tens of nanometers (Robbie et al., 1999). The columns are attached to the substrate on one end and may interact with neighboring columns through long-range forces. Based on this description of a columnar thin film, a discrete model has been constructed from a variety of components: a substrate, inextensible rods that model the columns, and springs that model the interaction between

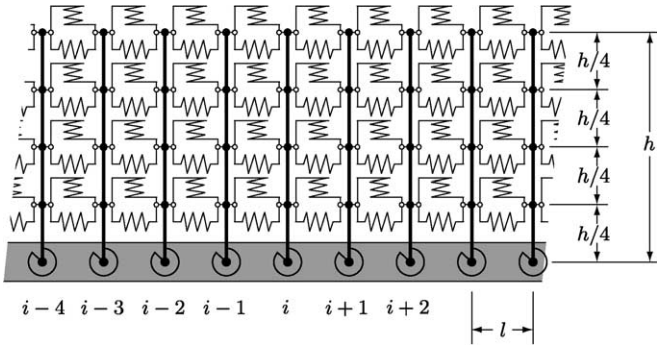

Fig. 1. The discrete model of a portion of a thin film with four spring pairs between each inextensible rod ($n = 4$) centered at the ith node. The spring pairs, separated by $h/4$ in the case shown here, are assumed to be acting at the point where they are attached to each rod (they are drawn in a schematic form in this figure). The choice of four spring pairs is simply shown as an example. In Section 3.1, the model will be formulated to account for an infinite number of springs.

the model's components. Fig. 1 shows a particular configuration of a central portion (excluding the boundaries) of such a discrete model.

The model shown in Fig. 1 is similar to a classical beam model in that it is defined over one dimension (horizontal in the figure) and is allowed to deform into two dimensions (horizontal and vertical). Before proceeding with a discussion of the components of the discrete model, it is necessary to present the kinematics of the model, which have been shown in Fig. 2. At each node i, there will be four independent displacement terms: u_i, v_i, ϕ_i, and β_i. Note that β_i is a relative rotation, since it is the rotation of the column relative to the rotation (or slope) of the substrate. For $\beta_i = 0$, the ith column is perpendicular to the substrate. In the initial configuration, as shown in Fig. 1, $u_i = v_i = 0$ and $\phi_i = \beta_i = 0$.

Keeping in mind the earlier physical description of a columnar thin film, it is now possible to associate an energy and deformation mechanisms with each of the components. First, in order to generate a linear system of governing equations, pairs of linear springs (harmonic potentials) are used to model the interaction between the columns. One spring accounts for the vertical displacement while another spring accounts for the horizontal displacement. In the discrete case, there will be n such pairs of springs (in the figures shown so far, $n = 4$). For the ith node, the contribution to the total strain energy due to these springs will be a function of each of the four displacements at each of the nodes $i - 1$, i, and $i + 1$, i.e., there will be 12

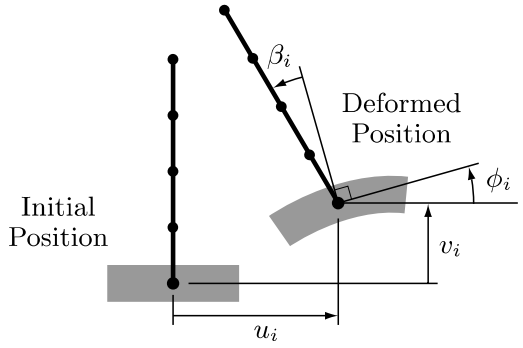

Fig. 2. There are four displacements describing the deformation of the ith node from the initial position to the deformed position: displacement in the horizontal direction, u_i; displacement in the vertical direction, v_i; rotation (or slope) of the substrate, ϕ_i; and rotation of the column relative to the substrate rotation, β_i.

discrete displacement terms appearing in the energy equation. Since the spring constants associated with vertical displacement are taken to be identical, they will be called k_1. Similarly, the spring constants associated with horizontal displacement will be called k_2 (see Fig. 3). The corresponding strain energy terms will be called U_1 and U_2, such that

$$(U_1)_i \equiv \frac{1}{2}k_1 \sum_{j=1}^{n} \left[(v_{i+1} - v_i)^2 + (v_i - v_{i-1})^2\right], \tag{2.1}$$

$$(U_2)_i \equiv \frac{1}{2}k_2 \sum_{j=1}^{n} \Big\{ \left[u_{i+1} - u_i - \lambda_j h(\beta_{i+1} + \phi_{i+1} - \beta_i - \phi_i)\right]^2 + \left[u_i - u_{i-1} - \lambda_j h(\beta_i + \phi_i - \beta_{i-1} - \phi_{i-1})\right]^2 \Big\}, \tag{2.2}$$

where

$$\lambda_j \equiv \frac{j}{n}, \tag{2.3}$$

and where we have used

$$\sin(\beta_i + \phi_i) \approx \beta_i + \phi_i, \qquad \cos(\beta_i + \phi_i) \approx 1. \tag{2.4}$$

Equations (2.4) are required to ensure that the resulting set of governing equations will be linear. For this reason, U_1 is not a function of β or ϕ terms. As an example, referring back to Fig. 1 where $n = 4$, Eqs. (2.1) and (2.2) would each consist of the sum of four terms, with the springs attached at points $h/4$, $h/2$, $3h/4$, and h along the length of the column. For the directed continuum version of the model to be presented in Section 3, n is considered to be infinite and the constants k_1 and k_2 will be scaled accordingly.

Next, the energy due to the torsional spring located at the ith node and described by spring constant k_3 is given by

$$(U_3)_i \equiv \frac{1}{2}k_3\beta_i^2. \tag{2.5}$$

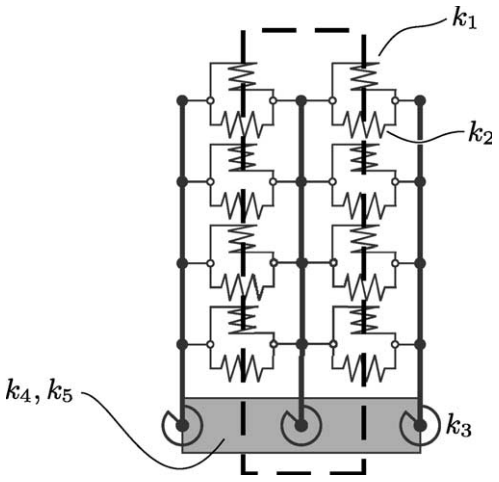

Fig. 3. A unit cell, enclosed by a dashed box, from the discrete model of the thin film with four spring pairs between each inextensible rod ($n = 4$). Note that there are $n = 4$ spring pairs consisting of $n = 4$ vertical springs (each with spring constant k_1) and $n = 4$ horizontal springs (each with spring constant k_2). The torsional springs are given by k_3 and the substrate is described by k_4 and k_5.

As has already been mentioned, when β_i equals zero, the column is perpendicular to the substrate. In this case, there is no twisting of the torsional spring and no contribution from the torsional spring to the total strain energy.

The final component of the discrete model to be considered is the substrate. Once again, to ensure linearity of the governing equations, it is necessary to treat the longitudinal deformation of the substrate independently from the bending of the substrate. The longitudinal deformation is modeled with a standard linear spring with spring constant k_4, such that, using previously established notation,

$$(U_4)_i \equiv \frac{1}{2}k_4\left[(u_{i+1}-u_i)^2+(u_i-u_{i-1})^2\right]. \tag{2.6}$$

The contribution to the strain energy due to bending will be a function of displacements v_{i-1}, v_i, v_{i+1}, ϕ_{i-1}, ϕ_i, and ϕ_{i+1} and material constant k_5, such that

$$\begin{aligned}(U_5)_i \equiv \frac{1}{2}k_5\Big\{&\left[3(v_{i+1}-v_i)^2-3l(\phi_i+\phi_{i+1})(v_{i+1}-v_i)+l^2(\phi_i^2+\phi_i\phi_{i+1}+\phi_{i+1}^2)\right]\\&+\left[3(v_i-v_{i-1})^2-3l(\phi_{i-1}+\phi_i)(v_i-v_{i-1})+l^2(\phi_{i-1}^2+\phi_{i-1}\phi_i+\phi_i^2)\right]\Big\}.\end{aligned} \tag{2.7}$$

The k_4 term of the energy function given in Eq. (2.6) is equivalent to an elastic bar subjected to tension or compression when k_4 is taken to equal EA/l, where EA is the equivalent stiffness of the rod. The k_5 term of the energy function given in Eq. (2.7) is equivalent to that for an Euler–Bernoulli beam when k_5 equals $4EI/l^3$, where EI is the bending stiffness of the beam. Although a beam is continuous, here it is treated in a discrete form so that it may be combined with the other discrete components of the model.

To clarify the differences between the substrate described by Eqs. (2.6) and (2.7) and a classical Euler–Bernoulli beam, it is worth noting that for an Euler–Bernoulli beam one assumes that the slope (given here by the ϕ terms) is equal to the first derivative of the displacement with respect to the horizontal position (in this work it would be v'). For an Euler–Bernoulli beam, one may think of ϕ as a constrained generalized coordinate and the relation $\phi = v'$ would be an additional constraint equation. With the addition of the spring elements k_1, k_2, and k_3 to the substrate as shown in Fig. 1, the resulting deformation ϕ will not necessarily equal v'.

Although the discrete model presented thus far was developed by considering the structure of columnar thin films, it may be useful to think about the model for use with other micro- and nano-scale systems. For example, the model exhibits non-local behavior, in a manner similar to Triantafyllidis and Bardenhagen (1993), because of the presence of the interacting columns attached at discrete nodes along the continuous substrate. The model may be thought of as a bilayer material, with the substrate as one layer and the interacting columns as another layer. It is hoped that the non-local model presented in the present work may be used to analyze other systems such as thin films with regular pores (Lew and Redwing, 2003), thin films with nano-voids (Mitra et al., 2004), nano-scale composite materials (Irie et al., 1997), multi-layered thin films (Wei et al., 2004), and micro-scale thin films in buckling (Volynskii et al., 2000, 2004,). Therefore, the model as presented thus far should be thought of more generally than simply as a model of a columnar thin film.

2.2. Formulating the discrete form of the governing equations

The goal now is to formulate the discrete form of the governing equations, i.e., the Lagrange's equations. Referring to the unit cell from Fig. 3, the total energy U is

$$U = U_0 + \sum_{i=1}^{m-1}\left[\frac{1}{2}(U_1)_i+\frac{1}{2}(U_2)_i+(U_3)_i+\frac{1}{2}(U_4)_i+\frac{1}{2}(U_5)_i\right]+U_m, \tag{2.8}$$

where U_0 denotes the energy associated with the left-hand half-cell and U_m denotes the energy of the right-hand half-cell. The one-half multiples in Eq. (2.8) are present since the unit cell includes one-half of the k_1,

k_2, k_4, and k_5 springs, as shown in Fig. 3. To write the discrete Lagrange's equations requires taking $4(m+1)$ derivatives, i.e., derivatives of the total energy U with respect to each of the displacements.

Since there are four displacements at $i=0$ and at $i=m$, there are $4(m-1)$ *interior* displacements. The governing equations presented in this work are based on the interior elements, and not the two boundaries, of the one-dimensional model. This is because the derivatives with respect to the displacements at $i=0$ and $i=m$ are different in form from the derivatives with respect to the interior displacements (see Eq. (2.8)). The $4(m-1)$ derivatives with respect to the interior displacements have the same form:

$$\frac{\partial U}{\partial u_i}=\frac{\partial (U_2)_i}{\partial u_i}+\frac{\partial (U_4)_i}{\partial u_i}=0,\quad i=1,2,\ldots,m-1, \tag{2.9}$$

$$\frac{\partial U}{\partial v_i}=\frac{\partial (U_1)_i}{\partial v_i}+\frac{\partial (U_5)_i}{\partial v_i}=0,\quad i=1,2,\ldots,m-1, \tag{2.10}$$

$$\frac{\partial U}{\partial \phi_i}=\frac{\partial (U_2)_i}{\partial \phi_i}+\frac{\partial (U_5)_i}{\partial \phi_i}=0,\quad i=1,2,\ldots,m-1, \tag{2.11}$$

$$\frac{\partial U}{\partial \beta_i}=\frac{\partial (U_2)_i}{\partial \beta_i}+\frac{\partial (U_3)_i}{\partial \beta_i}=0,\quad i=1,2,\ldots,m-1, \tag{2.12}$$

assuming that there are no external moments or forces applied, which is why the right-hand sides of Eqs. (2.9)–(2.12) equal zero. (This assumption is introduced since the purpose here is to demonstrate the feasibility of the model and not to analyze a particular case that may require such applied loads.) The results of the derivatives from Eqs. (2.9)–(2.12) applied to the energy terms given by Eqs. (2.1), (2.2) and (2.5)–(2.7) are

$$\begin{aligned}\frac{\partial U}{\partial u_i}&=k_2\sum_{j=1}^{n}\left[2u_i-u_{i-1}-u_{i+1}+\lambda_j h(\beta_{i-1}+\phi_{i-1}-2\beta_i-2\phi_i+\beta_{i+1}+\phi_{i+1})\right]\\&\quad+k_4(2u_i-u_{i-1}-u_{i+1}),\end{aligned} \tag{2.13}$$

$$\frac{\partial U}{\partial v_i}=k_1\sum_{j=1}^{n}(2v_i-v_{i-1}-v_{i+1})+\frac{3}{2}k_5\left[4v_i-2v_{i-1}-2v_{i+1}-l(\phi_{i-1}-\phi_{i+1})\right], \tag{2.14}$$

$$\begin{aligned}\frac{\partial U}{\partial \phi_i}&=k_2\sum_{j=1}^{n}\left[\lambda_j h(u_{i-1}-2u_i+u_{i+1})-(\lambda_j h)^2(\beta_{i+1}+\phi_{i+1}-2\beta_i-2\phi_i+\beta_{i-1}+\phi_{i-1})\right]\\&\quad+\frac{1}{2}k_5 l\left[3v_{i-1}-3v_{i+1}+l(4\phi_i+\phi_{i-1}+\phi_{i+1})\right],\end{aligned} \tag{2.15}$$

$$\frac{\partial U}{\partial \beta_i}=k_2\sum_{j=1}^{n}\left[\lambda_j h(u_{i-1}-2u_i+u_{i+1})-(\lambda_j h)^2(\beta_{i+1}+\phi_{i+1}-2\beta_i-2\phi_i+\beta_{i-1}+\phi_{i-1})\right]+k_3\beta_i, \tag{2.16}$$

where each of the derivatives equals zero according to Eqs. (2.9)–(2.12). After substituting λ_j from Eq. (2.3), the summations appearing in Eqs. (2.13)–(2.16) are observed to be convergent series of the forms

$$\sum_{j=1}^{n}\alpha=n\alpha,\quad \sum_{j=1}^{n}j\alpha=\frac{\alpha}{2}n(1+n),\quad \sum_{j=1}^{n}j^2\alpha=\frac{\alpha}{6}n(1+3n+2n^2), \tag{2.17}$$

for any constant α. After applying Eq. (2.17) to Eqs. (2.13)–(2.16), the final system of Lagrange's equations are

$$0=k_2\left[n(2u_i-u_{i-1}-u_{i+1})+\left(\frac{1+n}{2}\right)h(\beta_{i-1}+\phi_{i-1}-2\beta_i-2\phi_i+\beta_{i+1}+\phi_{i+1})\right]+k_4(2u_i-u_{i-1}-u_{i+1}), \tag{2.18}$$

$$0 = k_1 n(2v_i - v_{i-1} - v_{i+1}) + \frac{3}{2}k_5\left[4v_i - 2v_{i-1} - 2v_{i+1} - l(\phi_{i-1} - \phi_{i+1})\right], \tag{2.19}$$

$$0 = k_2\left[\left(\frac{1+n}{2}\right)h(u_{i-1} - 2u_i + u_{i+1}) - \left(\frac{1+3n+2n^2}{6n}\right)h^2(\beta_{i+1} + \phi_{i+1} - 2\beta_i - 2\phi_i + \beta_{i-1} + \phi_{i-1})\right] + \frac{1}{2}k_5 l\left[3v_{i-1} - 3v_{i+1} + l(4\phi_i + \phi_{i-1} + \phi_{i+1})\right], \tag{2.20}$$

$$0 = k_2\left[\left(\frac{1+n}{2}\right)h(u_{i-1} - 2u_i + u_{i+1}) - \left(\frac{1+3n+2n^2}{6n}\right)h^2(\beta_{i+1} + \phi_{i+1} - 2\beta_i - 2\phi_i + \beta_{i-1} + \phi_{i-1})\right] + k_3\beta_i. \tag{2.21}$$

3. Continuum model formulation

The goal of this section is to obtain the governing equations for a continuous system based on the discrete model with microstructural elements presented in Section 2. Ultimately, this goal will be accomplished by using Hamilton's principle, an energy minimization method, which requires a strain energy density function for the system. The advantage of this approach is that one obtains the complete BVP, i.e., both the governing equations in terms of continuous displacement functions $u(x)$, $v(x)$, $\phi(x)$, and $\beta(x)$ and the necessary boundary conditions. To obtain a strain energy density W for the desired continuous system based on the discrete system requires three steps:

(1) the discrete Lagrange's equations for the interior nodes, Eqs. (2.18)–(2.21), will be used to obtain continuous forms of the governing equations;
(2) the most general form of the quadratic homogeneous strain energy density will be formulated based on the kinematics of the directed continuum theory; and
(3) Hamilton's principle will be used to determine a reduced strain energy density by equating the resulting governing equations obtained from steps one and two of this procedure.

Once the reduced strain energy density is found, it will be used to determine the boundary conditions for the BVP.

3.1. Obtain continuous forms of the governing equations

The first step in the procedure is to obtain continuous versions of Eqs. (2.18)–(2.21). Following a common methodology (see Suiker et al., 2001), it is assumed that there are sufficiently smooth continuous functions of the position x that approximate the discrete displacement terms. It is then assumed that the displacement functions change gradually enough over the length $2l$ such that the discrete displacements at the nodes $i-1$ and $i+1$ may be written in terms of a Taylor series expansion of the displacement function evaluated at the ith node, where the position is given by x_i, in the following manner:

$$u_{i-1} \approx u(x_i) - lu'(x_i) + l^2u''(x_i)/2, \tag{3.1}$$

$$u_i = u(x_i), \tag{3.2}$$

$$u_{i+1} \approx u(x_i) + lu'(x_i) + l^2u''(x_i)/2, \tag{3.3}$$

where the prime notation indicates the derivative with respect to position $x \in (0, L)$ and L is the total length of the film. The form of Eqs. (3.1)–(3.3) is the same for the remaining displacements: v, ϕ, and β. The linear springs, the small angles assumptions used in Eq. (2.2), and the truncated Taylor series imply that the resulting model is restricted to the small deformation regime. Models that allow for large deformations will be presented in future work.

To obtain the desired form of the governing equations, the case with an infinite number of spring pairs between each inextensible rod will be considered, i.e., let $n \to \infty$ in the Lagrange's equations, Eqs. (2.18)–(2.21). It is necessary to scale the spring constants k_1 and k_2 by n, so that as $n \to \infty$ the overall stiffness of the system does not become infinite. Therefore, the following will be introduced into the Lagrange's equations:

$$k_1 = \hat{k}_1/n, \qquad k_2 = \hat{k}_2/n. \tag{3.4}$$

When these terms are used, the limit of the Lagrange's equations as $n \to \infty$ is determined. For example, after applying Eqs. (3.4) to Eq. (2.21), one obtains

$$\frac{\partial U}{\partial \beta_i} = \hat{k}_2\left[\left(\frac{1+n}{2n}\right)h(u_{i-1} - 2u_i + u_{i+1}) - \left(\frac{1+3n+2n^2}{6n^2}\right)h^2(\beta_{i+1} + \phi_{i+1} - 2\beta_i - 2\phi_i + \beta_{i-1} + \phi_{i-1})\right] + k_3\beta_i = 0, \tag{3.5}$$

such that the limit may be applied, i.e.,

$$\lim_{n\to\infty}\frac{\partial U}{\partial \beta_i} = \hat{k}_2\left[\frac{1}{2}h(u_{i-1} - 2u_i + u_{i+1}) - \frac{1}{3}h^2(\beta_{i+1} + \phi_{i+1} - 2\beta_i - 2\phi_i + \beta_{i-1} + \phi_{i-1})\right] + k_3\beta_i = 0. \tag{3.6}$$

Applying the Taylor series expansions of the displacement functions for all of the displacements, i.e., Eqs. (3.1)–(3.3) and the corresponding relations for v, ϕ, and β, applying the scaled spring constants introduced by Eqs. (3.4), and applying the limit procedure given by Eqs. (3.5) and (3.6) to Eqs. (2.18)–(2.21) leads to four second order linear homogeneous ordinary differential equations in the displacements

$$-\frac{1}{2}l^2\left\{2(\hat{k}_2 + k_4)u''(x) - h\hat{k}_2[\phi''(x) + \beta''(x)]\right\} = 0, \tag{3.7}$$

$$-l^2\left[(\hat{k}_1 + 3k_5)v''(x) - 3k_5\phi'(x)\right] = 0, \tag{3.8}$$

$$\frac{1}{6}l^2\left[3h\hat{k}_2u''(x) + (3l^2k_5 - 2h^2\hat{k}_2)\phi''(x) - 2h^2\hat{k}_2\beta''(x) - 18k_5v'(x) + 18k_5\phi(x)\right] = 0, \tag{3.9}$$

$$\frac{1}{2}hl^2\hat{k}_2u''(x) - \frac{1}{3}h^2l^2\hat{k}_2\phi''(x) - \frac{1}{3}h^2l^2\hat{k}_2\beta''(x) + k_3\beta(x) = 0. \tag{3.10}$$

Eqs. (3.7)–(3.10) may be rewritten in a form such that only one second order displacement function appears in each equation, which leads to

$$hl^2(\hat{k}_2 + 4k_4)u''(x) - 6k_3\beta(x) = 0, \tag{3.11}$$

$$(\hat{k}_1 + 3k_5)v''(x) - 3k_5\phi'(x) = 0, \tag{3.12}$$

$$l^4k_5\phi''(x) - 6l^2k_5v'(x) + 6l^2k_5\phi(x) - 2k_3\beta(x) = 0, \tag{3.13}$$

$$h^2l^4\hat{k}_2(\hat{k}_2 + 4k_4)k_5\beta''(x) + 6h^2l^2\hat{k}_2(\hat{k}_2 + 4k_4)k_5v'(x) - 6h^2l^2\hat{k}_2(\hat{k}_2 + 4k_4)k_5\phi(x) + 2k_3\left[h^2\hat{k}_2(\hat{k}_2 + 4k_4) - 6l^2(\hat{k}_2 + k_4)k_5\right]\beta(x) = 0. \tag{3.14}$$

The formulation of Eqs. (3.11)–(3.14) completes the first part of the previously outlined procedure to obtain the desired strain energy density function.

3.2. Obtain general form of the strain energy density

The second step of the procedure is to write a general form of the strain energy density. This general form will be based on the chosen kinematics and choice of directed continuum theory. Based on the results from Eqs. (3.11)–(3.14), it is apparent that there will be four independent displacement functions, $u(x)$, $v(x)$, $\phi(x)$, and $\beta(x)$, which are defined over the domain $x \in (0, L)$. Since there are four displacement functions for a one-dimensional domain, a micromorphic continuum theory, which is a particular case of directed continuum theories, will be used. Fig. 4 illustrates the columnar thin film model as described using a micromorphic continuum theory. The classical placement of points, described earlier as the placement of $\mathfrak{B}$ into $\mathcal{E}$, is denoted by $\boldsymbol{\chi}$ in the reference configuration and by $\mathbf{x}$ in the deformed configuration. The displacements $u(x)$ and $v(x)$ will be associated with the evolution of the body in the classical sense, where the displacement vector $\mathbf{u}(x)$ is defined in terms of the scalar displacement functions $u(x)$ and $v(x)$

$$\mathbf{u}(x) = u(x)\hat{\mathbf{e}}_1 + v(x)\hat{\mathbf{e}}_2. \tag{3.15}$$

The resulting displacement gradient H is defined in the standard way

$$\mathsf{H} = \nabla \mathbf{u}(x) = \begin{bmatrix} u'(x) & 0 \\ v'(x) & 0 \end{bmatrix}, \tag{3.16}$$

where the primes denote differentiation with respect to x and ∇ is the gradient operator. The right column contains zeros since u and v are only functions of x. Eq. (3.16) is shown as a 2×2 matrix only because this form is more typical in continuum mechanics derivations. For the model presented thus far, there is no physical meaning to derivatives with respect to any other position, i.e., other than x, since the domain of the present problem is one-dimensional. Since H is not constant, the deformation associated with H in Eq. (3.16) is not homogeneous.

The director in Fig. 4 is denoted by $\hat{\boldsymbol{\chi}}$ in the reference configuration (where it is a unit vector) and by $\hat{\mathbf{x}}$ in the deformed configuration. The deformation of $\hat{\boldsymbol{\chi}}$, whose components are taken to be the displacements $\phi(x)$ and $\beta(x)$, is associated with the evolution of the microstructure.[1] In the microstructure, the deformation of $\hat{\boldsymbol{\chi}}$ is taken to be homogeneous, although it is not homogeneous as a function of x. Therefore, it is possible to make use of the displacement gradient associated with the evolution of the microstructure, $\hat{\mathsf{H}}$, to relate $\hat{\mathbf{x}}$ to $\hat{\boldsymbol{\chi}}$, i.e.,

$$\hat{\mathbf{x}} = (\hat{\mathsf{H}} + \mathbf{I})\hat{\boldsymbol{\chi}}, \tag{3.17}$$

where $\boldsymbol{I}$ is the identity matrix. By making the same small angle assumptions that were given in Eqs. (2.4), it is possible to write

$$\hat{\mathsf{H}} = \begin{bmatrix} \beta(x) & -\phi(x) \\ \phi(x) & \beta(x) \end{bmatrix}, \tag{3.18}$$

which is to say that the unit vector $\hat{\boldsymbol{\chi}}$ rotates by the angle ϕ (where positive ϕ is a counter-clockwise rotation) and stretches by an amount β.

It is assumed that this material is hyperelastic, i.e., there exists a strain energy density function (per unit length in this case) called W that may be written as a function of strains. To obtain the general form of W,

[1] In the micromorphic theory, the director is capable of rotating and stretching, which is necessary in this case since there are two independent displacement functions to take into account. The two displacements $\phi(x)$ and $\beta(x)$ associated with the microstructure are obviously rotations. Since we have chosen to be consistent with the classical formulations of Mindlin and Eringen, in this work the rotation $\beta(x)$ will be viewed as a stretch of a unit vector, thus leading to a micromorphic theory. Identical results could be obtained by considering the displacements as a pair of rotations, in the sense of a micropolar theory with two rotating directors.

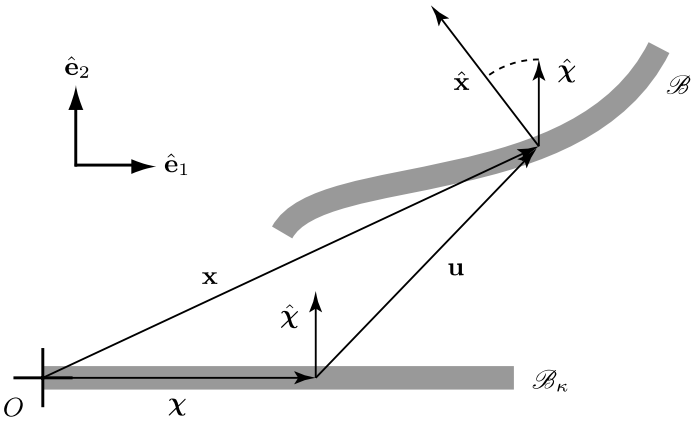

Fig. 4. Deformation of a thin film from $\boldsymbol{B}_\kappa$ (the reference configuration) to $\boldsymbol{B}$ (the deformed configuration) with one-dimensional domain in the horizontal direction given by $x \in (0, L)$, with unit vectors $\hat{e}_1$ and $\hat{e}_2$.

one must determine what constitutes the strain terms. Now that the displacement gradients have been given by Eqs. (3.16) and (3.18), the formulation of Mindlin (1964) will be used to obtain the strain terms. Mindlin defines three different strain tensors:

$$\mathsf{E} = \frac{1}{2}(\mathsf{H} + \mathsf{H}^{\mathrm{T}}), \qquad \Gamma = \mathsf{H}^{\mathrm{T}} - \hat{\mathsf{H}}, \qquad \mathsf{K} = \nabla\hat{\mathsf{H}}. \tag{3.19}$$

The purpose of Eqs. (3.19) is to identify the forms of the displacement functions that appear in the strain terms. By applying Eqs. (3.16) and (3.18) to Eqs. (3.19), it is apparent that there are six displacement function terms that appear in the strain tensors: $u'(x)$, $v'(x)$, $\phi(x)$, $\phi'(x)$, $\beta(x)$, and $\beta'(x)$. Based on Eqs. (3.19), $u'(x)$ and $v'(x)$ appear in E; $u'(x)$, $v'(x)$, $\phi(x)$, and $\beta(x)$ appear in Γ; and $\phi'(x)$ and $\beta'(x)$ appear in K. The most general quadratic homogeneous function of these six terms, and the general form of the strain energy density, is

$$\begin{aligned} W = {} & c_1 u'(x)^2 + c_2 v'(x)^2 + c_3 \phi(x)^2 + c_4 \phi'(x)^2 + c_5 \beta(x)^2 + c_6 \beta'(x)^2 + c_7 u'(x)v'(x) + c_8 u'(x)\phi(x) \\ & + c_9 u'(x)\phi'(x) + c_{10} u'(x)\beta(x) + c_{11} u'(x)\beta'(x) + c_{12} v'(x)\phi(x) + c_{13} v'(x)\phi'(x) + c_{14} v'(x)\beta(x) \\ & + c_{15} v'(x)\beta'(x) + c_{16}\phi(x)\phi'(x) + c_{17}\phi(x)\beta(x) + c_{18}\phi(x)\beta'(x) + c_{19}\phi'(x)\beta(x) \\ & + c_{20}\phi'(x)\beta'(x) + c_{21}\beta(x)\beta'(x), \end{aligned} \tag{3.20}$$

where the constants $c_1, c_2, \ldots, c_{21}$ are to be determined.

3.3. Obtain the reduced form of the strain energy density

To obtain the specific W based on the discrete model of Section 2, a general form of governing equations will be obtained via Hamilton's principle from W in Eq. (3.20). The general governing equations will be equated with those given by Eqs. (3.7)–(3.10) to solve for the constants $c_1, c_2, \ldots, c_{21}$ and thereby yield the reduced strain energy density function for the columnar thin film model. The total energy is given by the integral of the strain energy, i.e.,

$$U_t = \int_0^L W(u'(x), v'(x), \phi(x), \phi'(x), \beta(x), \beta'(x))\,\mathrm{d}x. \tag{3.21}$$

To minimize the definite integral in Eq. (3.21), it is necessary to consider the variation of U with respect to each of the four displacement fields (Lanczos, 1986) as

$$\delta U_t = \delta_u U_t + \delta_v U_t + \delta_\phi U_t + \delta_\beta U_t = 0. \tag{3.22}$$

It is according to Hamilton's principle that Eq. (3.22) is set to zero. After integrating by parts, one obtains the following for the four variations:

$$\delta_u U = \int_0^L \left(-\frac{\partial}{\partial x}\frac{\partial W}{\partial u'}\right)\delta u\,\mathrm{d}x + \frac{\partial W}{\partial u'}\delta u(x)\Big|_0^L, \tag{3.23}$$

$$\delta_v U = \int_0^L \left(-\frac{\partial}{\partial x}\frac{\partial W}{\partial v'}\right)\delta v\,\mathrm{d}x + \frac{\partial W}{\partial v'}\delta v(x)\Big|_0^L, \tag{3.24}$$

$$\delta_\phi U = \int_0^L \left(\frac{\partial W}{\partial \phi} - \frac{\partial}{\partial x}\frac{\partial W}{\partial \phi'}\right)\delta\phi\,\mathrm{d}x + \frac{\partial W}{\partial \phi'}\delta\phi(x)\Big|_0^L, \tag{3.25}$$

$$\delta_\beta U = \int_0^L \left(\frac{\partial W}{\partial \beta} - \frac{\partial}{\partial x}\frac{\partial W}{\partial \beta'}\right)\delta\beta\,\mathrm{d}x + \frac{\partial W}{\partial \beta'}\delta\beta(x)\Big|_0^L. \tag{3.26}$$

Each of the integrands in Eqs. (3.23)–(3.26) must equal zero for arbitrary variations δu, δv, $\delta\phi$, and $\delta\beta$. Therefore, each integrand is part of a single differential equation. By applying the general form of W from Eq. (3.20) to Eqs. (3.23)–(3.26), one obtains four general governing equations. By equating these resulting general governing equations with Eqs. (3.7)–(3.10), it is possible to obtain a reduced form of W; see Appendix A for details on this procedure. The strain energy density obtained by the variational approach is given by

$$\begin{aligned} W = \frac{1}{2}l^2\Big[&(\hat{k}_2 + k_4)u'(x)^2 + (\hat{k}_1 + 3k_5)v'(x)^2 + 3k_5\phi(x)^2 + \frac{1}{6}(2h^2\hat{k}_2 - 3l^2k_5)\phi'(x)^2 + k_3 l^{-2}\beta(x)^2 \\ &+ \frac{1}{3}h^2\hat{k}_2\beta'(x)^2 - h\hat{k}_2u'(x)\phi'(x) - h\hat{k}_2u'(x)\beta'(x) - 6k_5v'(x)\phi(x) + \frac{2}{3}h^2\hat{k}_2\phi'(x)\beta'(x)\Big]. \end{aligned} \tag{3.27}$$

The boundary conditions may either be given by specifying the displacements at the boundary (the essential boundary conditions) or by using the boundary terms of Eqs. (3.23)–(3.26) (the natural boundary conditions). As an example, $u(0)$ may be specified (in this case $\delta u(0) = 0$). If $u(0)$ is not specified, it will be assumed that no force is exerted on the boundary. Since the boundary term from Eq. (3.23) must equal zero, it means that $\partial W/\partial u'|_{x=0} = 0$. When natural boundary conditions are required, the derivatives obtained from the boundary terms of Eqs. (3.23)–(3.26) will be used. These derivatives are given by

$$\frac{\partial W}{\partial u'} = \frac{1}{2}l^2\Big[2(\hat{k}_2 + k_4)u' - h\hat{k}_2(\phi' + \beta')\Big], \tag{3.28}$$

$$\frac{\partial W}{\partial v'} = l^2\Big[(\hat{k}_1 + 3k_5)v' - 3k_5\phi\Big], \tag{3.29}$$

$$\frac{\partial W}{\partial \phi'} = \frac{1}{6}l^2\Big[-3h\hat{k}_2u' + (2h^2\hat{k}_2 - 3k_5l^2)\phi' + 2h^2\hat{k}_2\beta'\Big], \tag{3.30}$$

$$\frac{\partial W}{\partial \beta'} = \frac{1}{6}h\hat{k}_2l^2[-3u' + 2h(\beta' + \phi')]. \tag{3.31}$$

Therefore, the boundary value problem consists of the four second order ordinary differential equations given by Eqs. (3.11)–(3.14) and a combination of boundary conditions *either* given by Eqs. (3.28)–(3.31) *or* given by specifying the displacement at the boundary. Additional details utilizing the higher-order strain terms as given in Eqs. (3.19), the strain energy W, and the stress terms that are work-conjugates of the strain terms are presented in Appendix B.

4. Solving the system of governing equations

Before obtaining an analytical solution to the BVP as defined in Section 3, the BVP will be non-dimensionalized. The length term that all other length terms will be scaled by is l (see Fig. 1), which leads to these substitutions:

$$\xi \equiv x/l, \quad \tilde{u} \equiv u(\xi)/l, \quad \tilde{v} \equiv v(\xi)/l, \quad \tilde{\phi} \equiv \phi(\xi), \quad \tilde{\beta} \equiv \beta(\xi). \tag{4.1}$$

After applying Eqs. (4.1) to Eqs. (3.11)–(3.14), the governing equations may be completely non-dimensionalized by dividing each one through by a non-zero constant. In particular, Eq. (3.11) is divided through by $hl(\hat{k}_2 + 4k_4)$, Eq. (3.12) is divided through by $\hat{k}_1 + 3k_5$, Eq. (3.13) is divided through by $l^2 k_5$, and Eq. (3.14) is divided through by $h^2 l^2 \hat{k}_2(\hat{k}_2 + 4k_4)k_5$. When these steps are implemented, Eqs. (3.11)–(3.14) may be written in the non-dimensional form

$$0 = \tilde{u}''(\xi) - \kappa_1 \tilde{\beta}(\xi), \tag{4.2}$$

$$0 = \tilde{v}''(\xi) - \kappa_2 \tilde{\phi}'(\xi), \tag{4.3}$$

$$0 = \tilde{\phi}''(\xi) - 6\tilde{v}'(\xi) + 6\tilde{\phi}(\xi) - \kappa_3 \tilde{\beta}(\xi), \tag{4.4}$$

$$0 = \tilde{\beta}''(\xi) + 6\tilde{v}'(\xi) - 6\tilde{\phi}(\xi) + (\kappa_3 - \kappa_4)\tilde{\beta}(\xi), \tag{4.5}$$

where

$$\kappa_1 = \frac{6k_3}{h(\hat{k}_2 + 4k_4)l}, \tag{4.6}$$

$$\kappa_2 = \frac{3k_5}{\hat{k}_1 + 3k_5}, \tag{4.7}$$

$$\kappa_3 = \frac{2k_3}{k_5 l^2}, \tag{4.8}$$

$$\kappa_4 = \frac{12k_3(\hat{k}_2 + k_4)}{h^2 \hat{k}_2(\hat{k}_2 + 4k_4)}. \tag{4.9}$$

It is worth noting that κ_1, κ_2, κ_3, and κ_4 are all non-dimensional and that we have gone from five spring constants to four non-dimensional material constants. Before applying a similar technique to the natural boundary conditions, Eqs. (3.28)–(3.31), two additional non-dimensional terms must be introduced:

$$\Lambda \equiv L/l, \qquad \eta \equiv h/l, \tag{4.10}$$

where h is the discrete column length as shown in Fig. 1 and L is the total length. For this work, if the boundary displacements are not specified, it will be assumed that there are no loads or moments applied at the boundaries. Therefore, Eqs. (3.28)–(3.31) are set equal to zero and non-dimensionalized to yield the following four boundary conditions:

$$0 = \kappa_4 \tilde{u}' - \kappa_1 \left(\tilde{\phi}' + \tilde{\beta}'\right)\Big|_{\xi=0,\Lambda}, \tag{4.11}$$

$$0 = \tilde{v}' - \kappa_2 \tilde{\phi}|_{\xi=0,\Lambda}, \tag{4.12}$$

$$0 = \kappa_3 \left[-3\tilde{u}' + 2\eta\left(\tilde{\phi}' + \tilde{\beta}'\right)\right] - 2\eta\kappa_4 \tilde{\phi}'\Big|_{\xi=0,\Lambda}, \tag{4.13}$$

$$0 = -3\tilde{u}' + 2\eta\left(\tilde{\phi}' + \tilde{\beta}'\right)\Big|_{\xi=0,\Lambda}. \tag{4.14}$$

Of course, if the non-dimensionalized displacements are given instead, then the specified boundary displacements serve as the boundary conditions.

The continuous governing equations, Eqs. (4.2)–(4.5), are recast in first order form and solved analytically by calculating the Jordan canonical form (Coddington and Carlson, 1997). Four of the eight resulting eigenvalues are 0 and the remaining four eigenvalues are given by

$$\lambda = \pm\frac{1}{\sqrt{2}}\sqrt{6\kappa_2 - \kappa_3 + \kappa_4 - 6 \pm \sqrt{(6\kappa_2 - \kappa_3 + \kappa_4 - 6)^2 + 24(1-\kappa_2)\kappa_4}}. \tag{4.15}$$

From a physical perspective, all of the constants $\hat{k}_1$, $\hat{k}_2$, k_3, k_4, k_5, h, and l must be greater than zero. Based on Eqs. (4.6)–(4.9) it follows that $\kappa_1, \kappa_2, \kappa_3, \kappa_4 > 0$. In addition, based on Eq. (4.7), one may observe that $0 < \kappa_2 < 1$, which means that

$$\sqrt{(6\kappa_2 - \kappa_3 + \kappa_4 - 6)^2 + 24(1-\kappa_2)\kappa_4} > |\, 6\kappa_2 - \kappa_3 + \kappa_4 - 6 \,|, \tag{4.16}$$

so that Eq. (4.15) will always yield two real and two imaginary eigenvalues.

5. Some examples and results

The purpose of this section is to demonstrate some of the possible uses of the model presented in the preceding sections. In all of the cases to be analyzed, the film is subjected to the same type of loading, which is defined in Fig. 5. The horizontal displacements at each end ($\xi = 0$ and $\xi = \Lambda$) might be due to applied loads at each end, as a result of manufacturing induced stress in one of the layers of the film, or as a result of a mismatch in material properties, e.g., mismatch in coefficients of thermal expansion between two layers of a multi-layer film. Each end of the film is pinned so as to prevent vertical deflection. The remaining displacement functions, $\tilde{\phi}$ and $\tilde{\beta}$, are not constrained in any way. Therefore, the boundary conditions will consist of four essential boundary conditions

$$\tilde{u}(0) = \frac{\epsilon\Lambda}{2}, \quad \tilde{u}(\Lambda) = -\frac{\epsilon\Lambda}{2}, \quad \tilde{v}(0) = 0, \quad \tilde{v}(\Lambda) = 0, \tag{5.1}$$

and four natural boundary conditions

$$\tilde{\phi}'(0) = 0, \quad \tilde{\phi}'(\Lambda) = 0, \tag{5.2}$$

$$3\tilde{u}'(0) - 2\eta\tilde{\beta}'(0) = 0, \quad 3\tilde{u}'(\Lambda) - 2\eta\tilde{\beta}'(\Lambda) = 0, \tag{5.3}$$

where Eqs. (5.2) and (5.3) follow from Eqs. (4.13) and (4.14). (Eqs. (4.11) and (4.12) are not used here, since the actual displacements are given instead by Eqs. (5.1).) The non-dimensionalized constant ϵ is a loading parameter that specifies the horizontal displacement at the boundary. The various cases being studied are described by different values of κ_1, κ_2, κ_3, κ_4, Λ, and η. These constants are shown in Table 1. The numerical values were chosen to highlight different behavior observed from the model. They are also consistent with

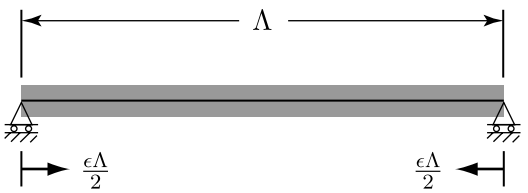

Fig. 5. The system to be analyzed consists of a film of non-dimensionalized length Λ subjected to horizontal displacements at each end of $\epsilon\Lambda/2$ and pinned to prevent vertical displacement. If $\epsilon > 0$, the film is compressed.

Table 1
The geometric and material constants that describe the directed continuum based model for the n cases considered in this section

Constant	Case 1	Case 2	Case 3	Case 4
κ_1	0.2	4	5.9	0.03
κ_2	0.999	0.916	0.098	0.098
κ_3	2	2.76	500	2.58
κ_4	0.2	10.5	11.2	0.0579
Λ	50	50	50	50
η	4	1.5	2	2
ϵ	0.02	0.02	0.02	0.02

Table 2
The four non-zero eigenvalues for each of the four cases

Case	Eigenvalues
1	$\lambda = \pm 1.344\mathrm{i}, \pm 0.02577$
2	$\lambda = \pm 0.8182\mathrm{i}, \pm 2.812$
3	$\lambda = \pm 22.23\mathrm{i}, \pm 0.3502$
4	$\lambda = \pm 2.824\mathrm{i}, \pm 0.1982$

Note that for each case there are two imaginary and two real valued non-zero eigenvalues.

the requirements discussed at the end of Section 4 regarding Eqs. (4.6)–(4.9). For completeness, the non-zero valued eigenvalues for all four cases are presented in Table 2.

5.1. Case 1—Euler–Bernoulli beam-like system

Case 1 is an example of how the directed continuum (DC) model approaches the classic Euler–Bernoulli (E–B) beam model. The vertical spring constant $\hat{k}_1$ is small compared with the other constants and h is larger than l. According to Eq. (4.7), it follows that κ_2 is close to 1, although it can never equal 1. In addition, according to Eqs. (4.6) and (4.9), both κ_1 and κ_4 are relatively small. The plots of the displacement functions for Case 1 are shown in Fig. 6. The similarity with an E–B beam is demonstrated by considering the

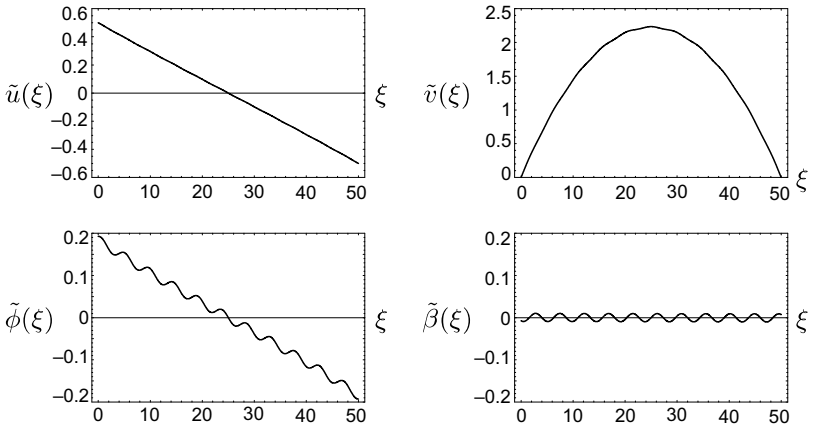

Fig. 6. Displacement fields for Case 1, the system most resembling the deformation of an Euler–Bernoulli beam.

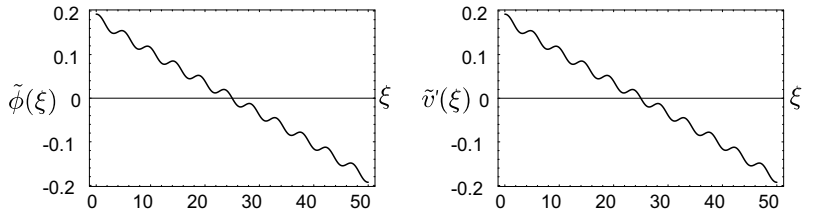

Fig. 7. Displacement fields $\tilde{\phi}(\xi)$ and $\tilde{v}'(\xi)$ for Case 1, the Euler–Bernoulli beam-like system. Note the similarity between these functions.

vertical displacement, $\tilde{v}(\xi)$. For an E–B beam with constant curvature, the vertical displacement function is quadratic. If one were to plot the quadratic best fit of $\tilde{v}(\xi)$ on Fig. 6, the two curves would be indistinguishable. The displacement $\tilde{\phi}(\xi)$ is also close to $\tilde{v}'(\xi)$ for this case, as shown in Fig. 7. (Recall that for an E–B beam, the derivative of the displacement is identified with the rotation of the cross-section of the beam.) In addition, the longitudinal displacement is linear. A linear displacement is the expected behavior of a rod or linear spring subjected to axial end loading conditions, where the governing equation would simply be given by $\tilde{u}''(\xi) = 0$, where $\tilde{u}(\xi)$ is the longitudinal displacement.

5.2. Case 2—oscillatory vertical deflection

The previous case considered a system whose behavior was similar to that expected for a classical E–B beam subjected to equal and opposite bending moments at both ends. In this case, we are considering a system with very different behavior. In fact, this case may be considered in light of the experimentally observed phenomenon of thin film buckling (Volynskii et al., 2000, 2004,). The results for this case, Case 2, are shown in Fig. 8. Clearly, the function $\tilde{v}(\xi)$ does not behave as an E–B beam (although, as in Case 1, $\tilde{\beta}(\xi)$ is smaller than $\tilde{\phi}(\xi)$). Both the wavelength and the amplitude of $\tilde{v}(\xi)$ change as the spring constants change. One of the areas to be investigated is the relationship between the wavelength of $\tilde{v}(\xi)$ and the material properties, which is a common issue of the buckling of thin films and coatings. It is worth noting that the wavelength for the DC model is independent of the loading parameter, given by ϵ, which is consistent with what is presented in the analysis of buckling using classical theories (Stafford et al., 2004).

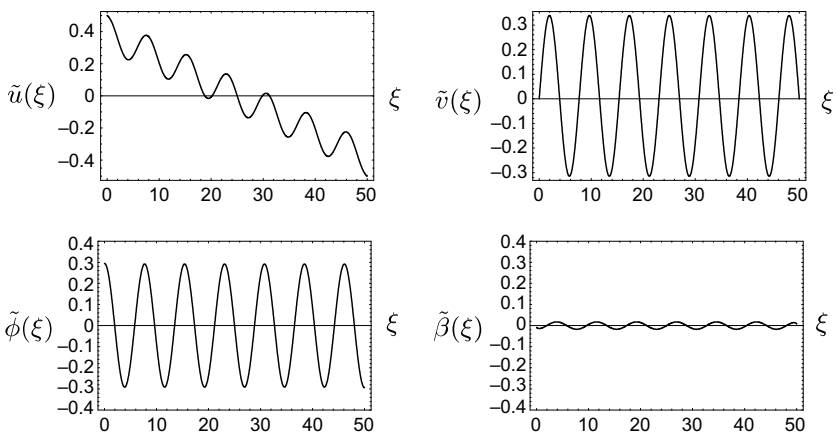

Fig. 8. Displacement fields for Case 2. In this case the material constants were chosen to produce an oscillatory vertical deflection, $\tilde{v}(\xi)$.

5.3. Case 3—flattened vertical deflection

Case 3, the results of which are shown in Fig. 9, produces a smooth, flattened deformation $\tilde{v}(\xi)$ that does not resemble the E–B beam behavior from Case 1. The fact that this system is quite different from a classical E–B beam is shown by Fig. 10. First, a quadratic fit is included along with the plot of $\tilde{v}(\xi)$. It is obvious that the DC model is not adequately described with an E–B beam subjected to bending load conditions. Second, $\tilde{v}'(\xi)$ is plotted with $\tilde{\phi}(\xi)$, showing that this system is unlike that of Case 1 and shown in Fig. 7. Also, because of the relative flexibility of the substrate in this system, rotation of the substrate matches very closely with the rotation of the columns, i.e., $\tilde{\beta}(\xi)$ is much smaller than $\tilde{\phi}(\xi)$. From the discrete model, when $\beta = 0$ the torsional spring does not rotate.

One way to consider the results presented thus far is by considering a possible use of this DC theory in the study of micro- and nano-scale thin films. Often, a stress is determined experimentally for a thin film by obtaining a single-valued measure of curvature. This is typically accomplished by focusing a laser along the surface of a thin film and measuring the change in the angle of deflection of the laser onto a detector device (Raghavan and Redwing, 2004). The relationship between a single value of curvature and a stress is usually expressed via the Stoney equation (Ohring, 1992), which is given as

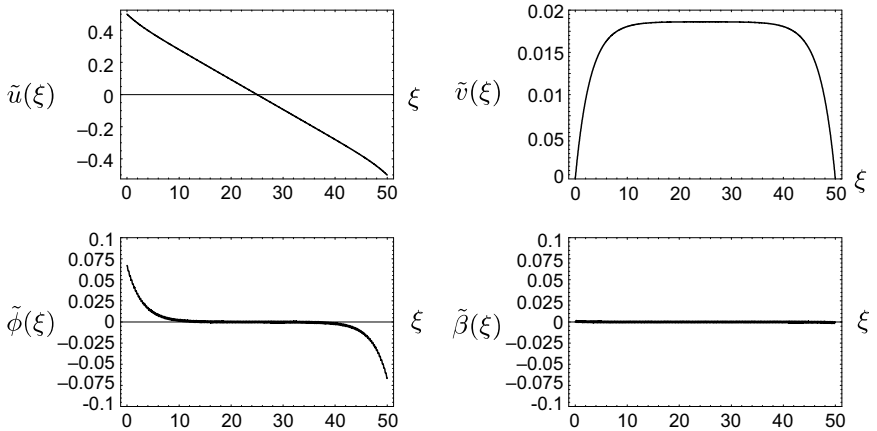

Fig. 9. The displacement fields for Case 3. The constants were chosen to produce a flattened vertical deflection, $\tilde{v}(\xi)$.

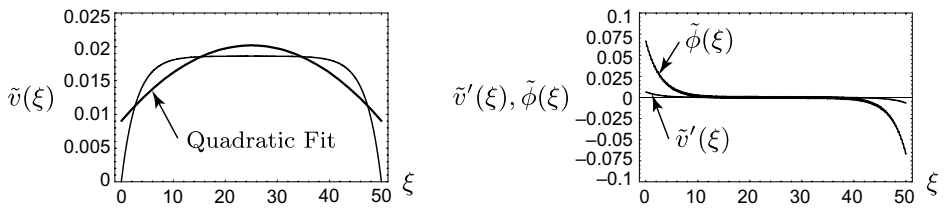

Fig. 10. In the left-hand plot, a quadratic fit of the vertical displacement $\tilde{v}(\xi)$ for Case 3 is included with the actual deformation for $\tilde{v}(\xi)$ from Fig. 9. The fit is associated with the behavior of an Euler–Bernoulli beam with a deformation described by a single valued curvature. Displacement fields $\tilde{\phi}(\xi)$ and $\tilde{v}'(\xi)$ are also shown in the right-hand plot. For an Euler–Bernoulli beam, these functions would be equal.

$$\sigma_f = \frac{1}{6R}\frac{E_s d_s^2}{(1-\nu_s)d_f}, \tag{5.4}$$

where E_s is the elastic modulus of the substrate, d_s is the thickness of the substrate, ν_s is the Poisson's ratio of the substrate, d_f is the thickness of the film, and R is the radius of curvature. The E–B beam theory gives a single value of curvature for a beam governed by the relation $v'''(x) = 0$, where the displacement v is given as a function of the position x along the length of the beam. If a thin film is modeled using such a theory, there will always be a constant R to be used with Eq. (5.4).

On the other hand, if the columnar structure of a thin film is modeled using a DC theory, it may be difficult to talk about a single curvature measurement for the entire film. Although the system as described by Case 1 may adequately be modeled using the Stoney equation, the results as shown in Fig. 10 for Case 3 demonstrate that any single value of R measured in an experiment would not represent the actual deflection of the thin film (compare the plot of $\tilde{v}(\xi)$ with the quadratic fit). Hence an estimate of the stress as given by Eq. (5.4) may not be representative of the actual physical system. Experimental observations of films with varying curvature are discussed in (Rosakis et al., 1998).

5.4. Case 4—reducing the torsional spring from case 3

The purpose of Case 4 is to consider the role of the torsional spring from the discrete model, described by k_3, on the overall behavior of the continuum model. This particular case, which may not be physically meaningful when considering actual columnar thin films, is included only to study the effect of the spring described by k_3. The presence of the torsional spring is critical in coupling the columnar structure to the substrate. The constants for this case were obtained by using the constants from Case 3 and only changing the value of k_3. Note that as k_3 becomes small, κ_3 also becomes small; see Eq. (4.8) and compare the value of κ_3 for Cases 3 and 4 in Table 1. The ability to exert a moment directly onto the substrate by the columnar structure is minimized since the torsional spring constant is minimized. The results for such a case are shown in Fig. 11. An immediate result of minimizing k_3, which is unlike the previous cases, is that $\tilde{\beta}(\xi)$ is no longer smaller than $\tilde{\phi}(\xi)$ (in fact, it is larger near the ends). Large scale oscillatory behavior is also introduced into $\tilde{v}(\xi)$ in a manner similar to that shown in Case 2. Finally, note that the average deformation of $\tilde{v}(\xi)$ is of the same order of magnitude of the deformation given in Case 3 (see Fig. 9).

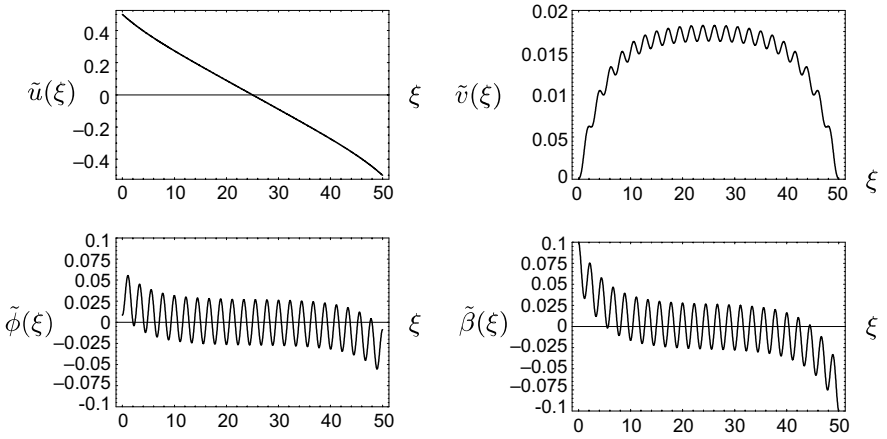

Fig. 11. Displacement fields for Case 4. The ability for the columnar structure to exert a bending moment on the substrate due to the rotation of the columns is minimized since the torsional spring constant, k_3, is small for this case.

6. Summary

The results, shown in Figs. 6–11 for the four cases, demonstrate the variety of physical responses possible due to a simple longitudinal deformation of a film as described using a directed continuum theory. It is suggested that the heterogeneous nature of the materials under consideration necessitates the use of higher-order theories, such as the micromorphic directed continuum theory presented thus far. Implementing such a theory has led to the formulation of a relatively simple system of linear ordinary differential equations. By moving from the discrete realm to the continuum realm, it is possible to better understand the problem by analyzing the strain energy density function and the governing differential equations.

It is hoped that this research will lead to more detailed models incorporating non-linear material behavior as well as kinetics. It will also be necessary to analyze actual physical systems, which requires the incorporation of actual material constants, geometric information, and a better understanding of the loading conditions into the model. A model thus formulated will be used in finite element calculations to simulate and predict the mechanical properties of a variety of micro- and nano-scale systems.

Acknowledgment

Partial support from the Air Force Office of Scientific Research through Grant No. F49620-02-1-0106 is gratefully acknowledged.

Appendix A. Determining the strain energy density

The purpose of this section is to obtain the strain energy density function W that was given in Eq. (3.27) from the general form given in Eq. (3.20). This will be done by applying Eq. (3.20) to Eqs. (3.23)–(3.26) to obtain a general form of the governing equations containing the terms $c_1, c_2, \ldots, c_{21}$. This general form of the governing equations will be equated with Eqs. (3.7)–(3.10) to obtain the constants $c_1, c_2, \ldots, c_{21}$.

Begin by applying Eq. (3.20) to Eq. (3.23). According to Hamilton's principle

$$-\frac{\partial}{\partial x}\frac{\partial W}{\partial u'} = -[2c_1u''(x) + c_7v''(x) + c_8\phi'(x) + c_9\phi''(x) + c_{10}\beta'(x) + c_{11}\beta''(x)] = 0. \tag{A.1}$$

Eq. (A.1) will be compared with Eq. (3.7), rewritten here,

$$-\frac{1}{2}l^2\left\{2(\hat{k}_2 + k_4)u''(x) - h\hat{k}_2[\phi''(x) + \beta''(x)]\right\} = 0, \tag{A.2}$$

and used to solve for the constants c_1, c_7, c_8, c_{10}, and c_{11}

$$c_1 = \frac{1}{2}l^2(\hat{k}_2 + k_4), \quad c_9 = c_{11} = -\frac{1}{2}hl^2\hat{k}_2, \quad c_7 = c_8 = c_{10} = 0. \tag{A.3}$$

In a similar manner, Eqs. (3.20) and (A.3) are applied to Eq. (3.24) to yield

$$-\frac{\partial}{\partial x}\frac{\partial W}{\partial v'} = -[2c_2v''(x) + c_{12}\phi'(x) + c_{13}\phi''(x) + c_{14}\beta'(x) + c_{15}\beta''(x)] = 0. \tag{A.4}$$

Eq. (3.8) is written here

$$-l^2\left[(\hat{k}_1 + 3k_5)v''(x) - 3k_5\phi'(x)\right] = 0, \tag{A.5}$$

to be compared with Eq. (A.4) to obtain solutions for c_2, c_{12}, c_{13}, c_{14}, and c_{15}

$$c_2 = \frac{1}{2} l^2(\hat{k}_1 + 3k_5), \quad c_{12} = -3l^2 k_5, \quad c_{13} = c_{14} = c_{15} = 0. \tag{A.6}$$

Eqs. (3.20), (A.3), and (A.6) are applied to Eq. (3.25), which leads to

$$\frac{\partial W}{\partial \phi} - \frac{\partial}{\partial x}\frac{\partial W}{\partial \phi'} = 2c_3\phi(x) - 2c_4\phi''(x) + \frac{1}{2}hl^2\hat{k}_2u''(x) - 3l^2k_5v'(x) + c_{17}\beta(x) + (c_{18} - c_{19})\beta'(x) - c_{20}\beta''(x) = 0. \tag{A.7}$$

Eq. (A.7) may be compared with Eq. (3.9), written here as

$$\frac{1}{6}l^2\left[3h\hat{k}_2u''(x) + (3l^2k_5 - 2h^2\hat{k}_2)\phi''(x) - 2h^2\hat{k}_2\beta''(x) - 18k_5v'(x) + 18k_5\phi(x)\right] = 0. \tag{A.8}$$

After comparing these equations, one finds that

$$c_3 = \frac{3}{2}l^2k_5, \quad c_4 = \frac{1}{12}l^2(2h^2\hat{k}_2 - 3l^2k_5), \quad c_{17} = 0, \tag{A.9}$$

$$c_{19} = c_{18}, \quad c_{20} = \frac{1}{3}h^2l^2\hat{k}_2. \tag{A.10}$$

Finally, Eqs. (3.20), (A.3), (A.6), (A.9) and (A.10) may be applied to Eq. (3.26) to obtain

$$\frac{\partial W}{\partial \beta} - \frac{\partial}{\partial x}\frac{\partial W}{\partial \beta'} = 2c_5\beta(x) - 2c_6\beta''(x) + \frac{1}{2}hl^2\hat{k}_2u''(x) - \frac{1}{3}h^2l^2\hat{k}_2\phi''(x) = 0. \tag{A.11}$$

Eq. (3.10) is rewritten here

$$\frac{1}{2}hl^2\hat{k}_2u''(x) - \frac{1}{3}h^2l^2\hat{k}_2\phi''(x) - \frac{1}{3}h^2l^2\hat{k}_2\beta''(x) + k_3\beta(x) = 0, \tag{A.12}$$

and is compared with Eq. (A.11) to show that

$$c_5 = \frac{1}{2}k_3, \quad c_6 = \frac{1}{6}h^2l^2\hat{k}_2. \tag{A.13}$$

From Eqs. (A.3), (A.6), (A.9), (A.10) and (A.13), it is apparent that the constants c_{16}, c_{18}, and c_{21} are arbitrary (keeping in mind that, according to Eq. (A.10), $c_{19} = c_{18}$). This means they may have any value and the governing equations that result will be identical to those given by Eqs. (3.7)–(3.10). These constants *will* appear in the natural boundary conditions, see Eqs. (3.25) and (3.26).

One way of determining the values of c_{16}, c_{18}, and c_{21}, and the method used in this work, is to reconsider the discrete form of the total energy given by Eq. (2.8). In particular, consider the energy of the interior nodes given by the summed terms from Eq. (2.8). In a manner similar to that used in Section 3, it is possible to generate a continuous form of the total energy. Since the highest order terms appearing in the energy density function are first order, the following expansion, see Eqs. (3.1)–(3.3), will be used

$$u_{i-1} \approx u(x_i) - lu'(x_i), \quad u_i = u(x_i), \quad u_{i+1} \approx u(x_i) + lu'(x_i), \tag{A.14}$$

where the form of Eqs. (A.14) is identical for the displacements v, ϕ, and β. Since Eq. (2.8) gives the discrete form of the total energy of the interior nodes, the continuous form of Eq. (2.8) will not be used directly, i.e., W is the strain energy density function and is not equivalent to Eq. (2.8). Rather, the continuous form of Eq. (2.8), obtained via Eqs. (A.14) and the equivalent expansions for the other displacements, will consist of some of the terms appearing in the general form of W given by Eq. (3.20). The presence or absence of quadratic strain terms will give us insight into our choice for the constants c_{16}, c_{18}, and c_{21}.

The summation from Eq. (2.8) consists of terms defined by Eqs. (2.1), (2.2), and (2.5),(2.6),(2.7). After applying the Taylor series expansion of the displacement function v evaluated at the ith node up to the

first order to Eq. (2.1), the resulting continuous equation includes the term $v'(x)^2$. After applying the necessary expansions to Eq. (2.2), the quadratic strain terms consist of the following: $u'(x)^2$, $\beta'(x)^2$, $\phi'(x)^2$, $u'(x)\phi'(x)$, $u'(x)\beta'(x)$, and $\phi'(x)\beta'(x)$. In a similar manner, the continuous form of Eq. (2.5) leads to the quadratic strain term $\beta(x)^2$ and the continuous form of Eq. (2.6) leads to $u'(x)^2$. Finally, after expanding the discrete displacements in Eq. (2.7), four quadratic strain terms result: $v'(x)^2$, $\phi(x)^2$, $\phi'(x)^2$, and $v'(x)\phi(x)$.

Note that the products $\phi(x)\phi'(x)$, $\phi(x)\beta'(x)$, $\phi'(x)\beta(x)$, and $\beta(x)\beta'(x)$ do not appear in the list of quadratic strain terms resulting from Eq. (2.8). Therefore, based on the energy from the discrete system, these terms will not be included in the final form of the strain energy function, i.e.,

$$c_{16} = c_{18} = c_{19} = c_{21} = 0. \tag{A.15}$$

In addition, consider the constants set to zero in Eqs. (A.3), (A.6), and (A.9): c_7, c_8, c_{10}, c_{13}, c_{14}, c_{15}, and c_{17}. The strain terms multiplied by these constants in Eq. (3.20) do not appear in the list of strain terms that result from Eq. (2.8).

After applying Eqs. (A.3), (A.6), (A.9) and (A.15) to Eq. (3.20), one obtains

$$W = \frac{1}{2}l^2\left[(\hat{k}_2 + k_4)u'(x)^2 + (\hat{k}_1 + 3k_5)v'(x)^2 + 3k_5\phi(x)^2 + \frac{1}{6}(2h^2\hat{k}_2 - 3l^2k_5)\phi'(x)^2 + k_3 l^{-2}\beta(x)^2 + \frac{1}{3}h^2\hat{k}_2\beta'(x)^2 - h\hat{k}_2u'(x)\phi'(x) - h\hat{k}_2u'(x)\beta'(x) - 6k_5v'(x)\phi(x) + \frac{2}{3}h^2\hat{k}_2\phi'(x)\beta'(x)\right]. \tag{A.16}$$

Eq. (A.16) is identical to Eq. (3.27).

Appendix B. Higher-order strain and stress terms

The purpose of this appendix is to develop the higher-order stress terms associated with micromorphic continuum theory. Beginning with Eqs. (3.19) and utilizing the strain energy density given by Eq. (3.27), the three work-conjugate stress terms will be defined. The balance of momenta relations of Mindlin (1964) will then be used to demonstrate the equivalence of the content of this appendix with Eqs. (3.7)–(3.10), (3.29)–(3.31), i.e., the governing equations and the boundary conditions.

From the definition of the strain tensors given by Eqs. (3.19) and the definitions of H and $\hat{\mathsf{H}}$ given by Eqs. (3.16) and (3.18), it follows that

$$\mathsf{E} = \begin{bmatrix} u'(x) & v'(x)/2 \\ v'(x)/2 & 0 \end{bmatrix} = \begin{bmatrix} E_{11} & E_{12} \\ E_{21} & E_{22} \end{bmatrix}, \tag{B.1}$$

$$\mathsf{\Gamma} = \begin{bmatrix} u'(x) - \beta(x) & v'(x) + \phi(x) \\ -\phi(x) & -\beta(x) \end{bmatrix} = \begin{bmatrix} \Gamma_{11} & \Gamma_{12} \\ \Gamma_{21} & \Gamma_{22} \end{bmatrix}, \tag{B.2}$$

$$\{\mathsf{K}\}_1 = \begin{bmatrix} \beta'(x) & -\phi'(x) \\ \phi'(x) & \beta'(x) \end{bmatrix} = \begin{bmatrix} K_{111} & K_{112} \\ K_{121} & K_{122} \end{bmatrix}, \tag{B.3}$$

where the subscript attached to the third order tensor K signifies that only the derivatives with respect to x will be considered since all other derivatives must equal zero. The homogeneous quadratic potential energy density function that is identical to Eq. (3.27) may be written as

$$W = \frac{1}{2}\mathbf{e}^{\mathrm{T}}\mathbf{C}\mathbf{e} + \frac{1}{2}\boldsymbol{\gamma}^{\mathrm{T}}\mathbf{B}\boldsymbol{\gamma} + \frac{1}{2}\mathbf{k}^{\mathrm{T}}\mathbf{A}\mathbf{k} + \boldsymbol{\gamma}^{\mathrm{T}}\mathbf{D}\mathbf{k} + \mathbf{k}^{\mathrm{T}}\mathbf{F}\mathbf{e} + \boldsymbol{\gamma}^{\mathrm{T}}\mathbf{G}\mathbf{e}, \tag{B.4}$$

where the vectors $\boldsymbol{e}$, $\boldsymbol{\gamma}$, and $\boldsymbol{k}$ are defined as

$$\mathbf{e} = \begin{Bmatrix} E_{11} \\ E_{22} \\ E_{12} \\ E_{21} \end{Bmatrix}, \quad \boldsymbol{\gamma} = \begin{Bmatrix} \Gamma_{11} \\ \Gamma_{22} \\ \Gamma_{12} \\ \Gamma_{21} \end{Bmatrix}, \quad \mathbf{k} = \begin{Bmatrix} K_{111} \\ K_{122} \\ K_{112} \\ K_{121} \end{Bmatrix}. \tag{B.5}$$

These vectors simply contain the terms found in the strain tensors in Eqs. (B.1)–(B.3). The six 4 by 4 matrices from Eq. (B.4) are defined as follows:

$$\mathbf{C} = \begin{bmatrix} (\hat{k}_2 + k_4)l^2 & 0 & 0 & 0 \\ 0 & 0 & 0 & 0 \\ 0 & 0 & (\hat{k}_1 + 12k_5)l^2 & (\hat{k}_1 + 12k_5)l^2 \\ 0 & 0 & (\hat{k}_1 + 12k_5)l^2 & (\hat{k}_1 + 12k_5)l^2 \end{bmatrix}, \tag{B.6}$$

$$\mathbf{B} = \begin{bmatrix} 0 & k_3 & 0 & 0 \\ k_3 & -k_3 & 0 & 0 \\ 0 & 0 & 3k_5 l^2 & 0 \\ 0 & 0 & 0 & 0 \end{bmatrix}, \tag{B.7}$$

$$\mathbf{A} = \begin{bmatrix} h^2\hat{k}_2 l^2/3 & 0 & -h^2\hat{k}_2 l^2/3 & 0 \\ 0 & 0 & 0 & 0 \\ -h^2\hat{k}_2 l^2/3 & 0 & (h^2\hat{k}^2/3 - k_5 l^2/2)l^2 & 0 \\ 0 & 0 & 0 & 0 \end{bmatrix}, \tag{B.8}$$

$$\mathbf{F} = \begin{bmatrix} -h\hat{k}_2 l^2/2 & 0 & 0 & 0 \\ 0 & 0 & 0 & 0 \\ h\hat{k}_2 l^2/2 & 0 & 0 & 0 \\ 0 & 0 & 0 & 0 \end{bmatrix}, \tag{B.9}$$

$$\mathbf{G} = \begin{bmatrix} 0 & 0 & 0 & 0 \\ -k_3 & 0 & 0 & 0 \\ 0 & 0 & -6k_5 l^2 & -6k_5 l^2 \\ 0 & 0 & 0 & 0 \end{bmatrix}, \tag{B.10}$$

and **D** is the zero matrix. Due to the presence of the matrix $\boldsymbol{F}$, this continuum model is anisotropic. After substituting Eqs. (B.1)–(B.3) and (B.5)–(B.10) with **D = 0** into Eq. (B.4), one obtains a strain energy density identical to that given by Eq. (3.27).

There are three stress tensors that are the work-conjugates of the strain tensors, referred to by Mindlin as the Cauchy stress, the relative stress, and the double stress, respectively:

$$\mathsf{T} \equiv \frac{\partial W}{\partial \mathsf{E}} = \mathsf{T}^{\mathrm{T}}, \quad \Sigma = \frac{\partial W}{\partial \boldsymbol{\Gamma}}, \quad \mathsf{M} = \frac{\partial W}{\partial \mathsf{K}}, \tag{B.11}$$

where the symmetry of the Cauchy stress follows from the symmetry of $\boldsymbol{E}$. Based on Eq. (B.4), the components of the stress tensors are

$$\{\mathsf{T}\}_{11} = k_3\beta(x) + (\hat{k}_2 + k_4)l^2 u'(x) - \frac{1}{2}h\hat{k}_2 l^2 \beta'(x) - \frac{1}{2}h\hat{k}_2 l^2 \phi'(x), \tag{B.12}$$

$$\{\mathsf{T}\}_{12} = \{\mathsf{T}\}_{21} = -6k_5 l^2 \phi(x) + (\hat{k}_1 + 6k_5)l^2 v'(x), \tag{B.13}$$

$$\{\mathsf{T}\}_{22} = 0, \tag{B.14}$$

$$\{\Sigma\}_{11} = -k_3\beta(x), \tag{B.15}$$

$$\{\Sigma\}_{12} = 3k_5 l^2\phi(x) - 3k_5 l^2 v'(x), \tag{B.16}$$

$$\{\Sigma\}_{21} = \{\Sigma\}_{22} = 0, \tag{B.17}$$

$$\{\mathsf{M}\}_{111} = -\frac{1}{2}h\hat{k}_2 l^2 u'(x) + \frac{1}{3}h^2\hat{k}_2 l^2\beta'(x) + \frac{1}{3}h^2\hat{k}_2 l^2\phi'(x), \tag{B.18}$$

$$\{\mathsf{M}\}_{112} = \frac{1}{2}h\hat{k}_2 l^2 u'(x) - \frac{1}{3}h^2\hat{k}_2 l^2\beta'(x) - \frac{1}{3}h^2\hat{k}_2 l^2\phi'(x) + \frac{1}{2}k_5 l^4\phi'(x), \tag{B.19}$$

$$\{\mathsf{M}\}_{121} = \{\mathsf{M}\}_{122} = 0. \tag{B.20}$$

For the static case under consideration, the balance of momenta equations that result from the variation of the strain energy density given by Mindlin (1964) are rewritten as

$$\mathrm{Div}(\mathsf{T} + \Sigma) + \mathbf{f} = 0, \qquad \mathrm{Div}\mathsf{M} + \Sigma + \Phi = 0, \tag{B.21}$$

where $\boldsymbol{f}$ is the body force per unit volume and Φ is the double force per unit volume. In the present analysis, there are neither body forces nor double forces present. The boundary conditions are given using the traction $\boldsymbol{t}$ and double force per unit area Θ as

$$\mathbf{t} = (\mathsf{T} + \Sigma)\mathbf{n}, \qquad \Theta = \mathsf{M}\mathbf{n}, \tag{B.22}$$

where $\boldsymbol{n}$ is the unit vector normal to the surface. Applying Eqs. (B.12)–(B.20) to Eqs. (B.21) yields the four governing equations, given by Eqs. (3.7)–(3.10). Applying these same relations to Eqs. (B.22) yields the four natural boundary conditions as given by Eqs. (3.28)–(3.31) when $\boldsymbol{t} = 0$ and $\Theta = 0$.

References

Askar, A., Cakmak, A., 1968. A structural model of a micropolar continuum. International Journal of Engineering Science 6, 583–589.

Bažant, Z.P., 1971. Micropolar medium as a model for buckling of grid frameworks. In: Lee, L.N., Szewczyk, A.A. (Eds.), 12th Midwestern Mechanics Conference. Developments in Mechanics, Vol. 6. University of Notre Dame Press, Notre Dame, IN.

Bažant, Z.P., Christensen, M., 1972. Analogy between micropolar continuum and grid frameworks under initial stress. International Journal of Solids and Structures 8 (3), 327–346.

Capriz, G., Podio-Guidugli, P., 1976. Discrete and continuous bodies with affine structure. Annali di Matematica Pura ed Applicata 111, 195–211.

Coddington, E.A., Carlson, R., 1997. Linear Ordinary Differential Equations. Society for Industrial and Applied Mathematics, Philadelphia.

Eringen, A.C., 1966. Linear theory of micropolar elasticity. Journal of Mathematics and Mechanics 15 (6), 909–923.

Eringen, A.C., 1968. Theory of micropolar elasticity. In: Mathematical Fundamentals. Fracture: an Advanced Treatise, Vol. 2. Academic Press, New York, London, pp. 621–729.

Huang, R., 2004. Kinetic wrinkling of an elastic film on a viscoelastic substrate. Tech. Rep. 04/01, Research Center for Mechanics of Solids, Structures, & Materials—The University of Texas.

Irie, M., Ohara, H., Nakayama, A., Kitagawa, N., Nomura, T., 1997. Deposition of Ni–TiN nano-composite films by cathodic arc ion-plating. Nuclear Instruments and Methods in Physics Research Section B—Beam Interactions with Materials and Atoms 121 (1–4), 133–136.

Koiter, W.T., 1964. Couple-stresses in the theory of elasticity. I. Proceedings of the Royal Netherlands Academy of Sciences—Series B: Physical Sciences 67 (1), 17–29.

Lanczos, C., 1986. The Variational Principles of Dynamics. Dover, New York.

Lew, K.K., Redwing, J.M., 2003. Growth characteristics of silicon nanowires synthesized by vapor–liquid–solid growth in nanoporous alumina templates. Journal of Crystal Growth 254 (1-2), 14–22.

Mindlin, R.D., 1964. Micro-structure in linear elasticity. Archive for Rational Mechanics and Analysis 16, 51–78.

Mitra, R., Chiou, W.A., Weertman, J.R., 2004. In situ study of deformation mechanisms in sputtered free-standing nanocrystalline nickel films. Journal of Materials Research 19 (4), 1029–1037.

Ohring, M., 1992. The Materials Science of Thin Films. Academic Press, San Diego.

Raghavan, S., Redwing, J.M., 2004. In situ stress measurements during MOCVD growth of AlN buffer layers on (1 1 1) Si substrates. Journal of Crystal Growth 261, 294–300.

Robbie, K., Shafai, C., Brett, M.J., 1999. Thin films with nanometer-scale pillar microstructure. Journal of Materials Research 14 (7), 3158–3163.

Rosakis, A., Singh, R., Tsuji, Y., Kolawa, E., Moore, N., 1998. Full field measurements of curvature using coherent gradient sensing: Applications to thin film characterization. Thin Solid Films 325, 42–54.

Stafford, C., Harrison, C., Beers, K., Karim, A., Amis, E., Vanlandingham, M., Kim, H.-C., Volksen, W., Miller, R., Simonyi, E., 2004. A buckling-based metrology for measuring the elastic moduli of polymeric thin films. Nature Materials.

Suiker, A.S.J., Metrikine, A.V., de Borst, R., 2001. Comparison of wave propagation characteristics of the Cosserat continuum model and corresponding discrete lattice models. International Journal of Solids and Structures 38 (9), 1563–1583.

Toupin, R.A., 1964. Theories of elasticity with couple-stress. Archive for Rational Mechanics and Analysis 17, 85–112.

Triantafyllidis, N., Bardenhagen, S., 1993. On higher-order gradient continuum-theories in 1-D nonlinear elasticity; Derivation from and comparison to the corresponding discrete models. Journal of Elasticity 33 (3), 259–293.

Truesdell, C., Noll, W., 2003. The Non-linear Field Theories of Mechanics, Third ed. Springer-Verlag, Berlin.

Volynskii, A., Bazhenov, S., Lebedeva, O., Bakeev, N., 2000. Mechanical buckling instability of thin coatings deposited on soft polymer substrates. Journal of Materials Science 35, 547–554.

Wei, G.H., Bhushan, B., Jacobs, S.J., 2004. Nanomechanical characterization of multilayered thin film structures for digital micromirror devices. Ultramicroscopy 100 (3-4), 375–389.